PHYSICAL REVIEW B **89**, 121118(R) (2014)

Ferromagnetic response of a "high-temperature" quantum antiferromagnet

Xin Wang,[1] Rajdeep Sensarma,[2] and Sankar Das Sarma[1]
[1]*Condensed Matter Theory Center, Department of Physics, University of Maryland, College Park, Maryland 20742, USA*
[2]*Department of Theoretical Physics, Tata Institute of Fundamental Research, Mumbai 400005, India*
(Received 14 August 2013; revised manuscript received 24 February 2014; published 31 March 2014)

We study the finite-temperature antiferromagnetic phase of the ionic Hubbard model in the strongly interacting limit using quantum Monte Carlo based dynamical mean-field theory. We find that the ionic potential plays a dual role in determining the antiferromagnetic order. A small ionic potential (compared to Hubbard repulsion) increases the superexchange coupling in the projected sector of the model, leading to an increase in the Neel temperature of the system. A large ionic potential leads to resonance between projected antiferromagnetically ordered configurations and density ordered configurations with double occupancies, thereby killing antiferromagnetism in the system. This novel way of degrading antiferromagnetism leads to spin polarization of the low-energy single-particle density of states. The dynamic response of the system thus mimics ferromagnetic behavior, although the system is still an antiferromagnet in terms of the static spin order.

DOI: 10.1103/PhysRevB.89.121118 PACS number(s): 75.10.−b, 67.85.−d, 72.25.−b

Ultracold atoms in optical lattices [1] have emerged as a novel platform for strongly correlated physics, where lattice models, relevant to condensed matter systems and other arenas of physics, can be implemented and studied in a controllable way [2–5]. The easy tunability of the Hamiltonian parameters and the accurate knowledge and control of the underlying parameters have made these systems the foremost candidate for emulating models like the repulsive Bose and Fermi-Hubbard models, which are routinely used as paradigms in the study of correlation-driven superfluid-insulator transitions [6] and high-temperature superconductors [7]. In fact, a whole new subject at the interface of condensed matter and atomic physics has emerged in this context, being dubbed 'optical lattice emulation" (OLE).

The implementation of the Fermi-Hubbard model [3,4] in the strongly interacting limit has raised the prospect of observing antiferromagnetic (AF) spin ordering in these systems [3]. At present, observing antiferromagnetism with cold atoms is a major goal of experimentalists, which would be a stepping stone towards observation of the more complicated phenomenon of high-temperature superconductivity. While the basic mechanism of superexchange has been verified in cold atom experiments [8], spontaneous AF ordering is yet to be seen in optical lattices. The main problem is that the temperature scale for the AF transition is simply too low to be achievable in the laboratory at the present time [9]. While a lot of effort has been spent towards improving cooling techniques in optical lattices [10], in this Rapid Communication, we propose a different way of observing AF ordering, by modifying the lattice model in a way that the Neel temperature is higher than that of the standard Fermi-Hubbard model. A similar approach has been used to study "magnetism" in a system with an effective electric field on the atoms [11]. However, the magnetism in that case is driven by the hopping of fermions [12] and throws little light on superexchange-dominated AF order, which is of key interest in the context of strong correlation physics.

We study a related model called the ionic Hubbard model, which was first introduced in the context of the ionic to neutral transition of charge transfer organic compounds [13,14]. In addition to hopping of the fermions on a bipartite lattice and the usual on-site Hubbard repulsion, the fermions on the different sublattices feel different local potential energies, which breaks the sublattice symmetry in the "charge" sector. This model can be easily implemented in a cold atom setting, with the staggered local potential being imprinted using holographic techniques [15]. In the strongly interacting limit, we find that the effective superexchange scale, and hence the AF transition temperature at half filling, increases with the ionic potential. This should make it easier to see AF order in this model as compared with the standard fermionic Hubbard model. We find that the Neel temperature can be enhanced by about 40% for reasonable values of the parameters.

In the ionic Hubbard model, when the staggered potential is comparable to the Hubbard repulsion, we find that the low-energy single-particle density of states (DOS) for the up ($\uparrow$) and down ($\downarrow$) spins are different, i.e., the system shows ferromagnetic characteristics in its low-frequency dynamics, although it continues to exhibit static AF order. This counterintuitive result is understood as an effect of the interplay between the bichromatic nature of the lattice and the AF order in the system. This surprising result can be confirmed by either polarization-dependent rf spectroscopy [16] or spin conductivity [17] or spin injection spectroscopy [18] measurements.

The ionic Hubbard model is defined on a bipartite lattice (e.g., a square or a cubic lattice with two sublattices A and B) as

$$H = -t \sum_{\langle ij \rangle} c^{\dagger}_{i\sigma} c_{j\sigma} + U \sum_{i} n_{i\uparrow} n_{i\downarrow} + \frac{V}{2} \sum_{i} (-1)^{\gamma_i} n_i, \quad (1)$$

where t is the nearest neighbor hopping matrix element, U the local Hubbard repulsion, $\gamma_i = 1(0)$ if i is a site on A (B) sublattice, and V is the amplitude of the staggered ionic potential. This model has a rich phase diagram as temperature, carrier density, the interaction parameter U/t or the ionic potential V/U are tuned [13,14,19–24].

In this Rapid Communication, we solely focus on the system at half filling, i.e., one particle per lattice site. In the noninteracting limit ($U = 0$), the system is a band insulator (since the staggered potential doubles the unit cell). In the strongly interacting limit ($U \gg V,t$), the system is an AF Mott

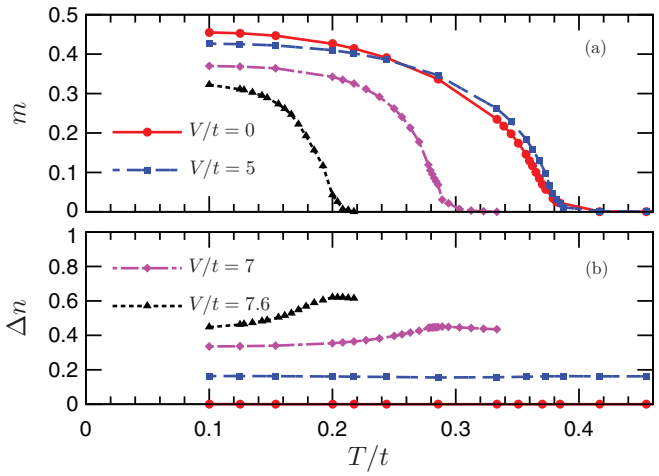

FIG. 1. (Color online) (a) Staggered magnetization m and (b) difference in density between A and B sublattices Δn as functions of temperature for different values of the ionic potential V. The Hubbard interaction is fixed at $U/t = 10$ for all the plots.

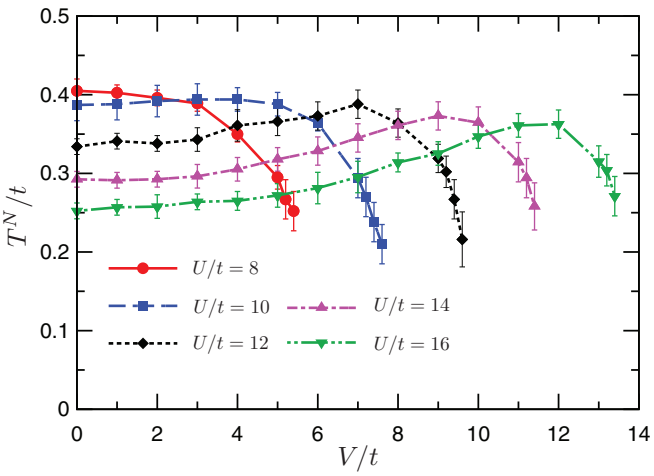

FIG. 2. (Color online) Dependence of the Neel temperature T^N on the ionic potential V/t for several different values of the Hubbard interaction U. At large U/t, the Neel temperature initially rises with V/t before crashing down.

insulator, with the spin ordering governed by a superexchange scale $J = 4t^2/U$. Most of the previous studies [13,14,19–24] on the system have focused on how the system goes from a band to a Mott insulator and whether there is an intervening metallic phase, while the antiferromagnetic phase has been studied at weak coupling [25,26]. Our work has a completely different focus. Starting from the interaction-dominated limit ($V = 0$, $U/t \gg 1$), we are interested in the fate of the spin ordering in the system as a function of the temperature and the staggered potential V/U.

We use the dynamical mean-field theory (DMFT) [27] together with a quantum Monte Carlo impurity solver [28] to study the AF ordered phase of this model. DMFT approximates the interacting lattice problem by a single site or a small cluster (i.e., impurities) interacting with a bath. The dynamics of the bath and the impurities are then solved self-consistently to obtain the local Green's functions for the interacting problem, which are used to calculate various properties of the system. Since we are interested in the spin dynamics in the presence of an explicitly broken sublattice symmetry, the local Green's functions include $G^{\uparrow(\downarrow)}_{A(B)}(\tau)$, where $G^{\sigma}_{\alpha}(\tau)$ is the imaginary-time Green's function of the fermions with spin σ on sublattice α. We first obtain an AF state at $V = 0$, after which we slowly turn on V. We typically take at least 10^9 Monte Carlo steps in each iteration, and for certain cases, more than 60 iterations are used to ensure convergence. We note that as a method, DMFT is exact in infinite dimensions. For hypercubic lattices, DMFT calculations are expected to better capture the qualitative and quantitative features of the model [27] as the dimension increases, which, for cold atom systems, can at best take the value of 3.

We first focus our attention on the AF ordering in the system. The density of each spin on each sublattice is given by $n^{\sigma}_{\alpha} = 1 + G^{\sigma}_{\alpha}(\tau \to 0^+)$, while the staggered magnetization m, characterizing the AF order, is given by $m = (n^{\uparrow}_A + n^{\downarrow}_B - n^{\downarrow}_A - n^{\uparrow}_B)/4$. The dependence of m on temperature for different values of V/t (for a fixed $U/t = 10$) is plotted in Fig. 1(a). The magnetization decreases with temperature and vanishes at the Neel temperature T^N. As V/t is raised to around 7 and beyond, the magnetization (at a given temperature) is sharply suppressed with increasing V/t, and T^N also varies rapidly with V/t in this regime.

The Neel temperature is plotted as a function of V/t for several values of U/t in Fig. 2. Up to $U/t = 10$, T^N is a monotonically decreasing function of V/t. For $U/t = 12$, T^N first rises as a function of V/t, reaches a maximum, and then crashes as V/t is increased farther. For $U/t > 12$, this effect is much more pronounced. This nonmonotonic behavior of T^N at strong coupling can be understood by the following perturbative argument. For large U/t and small V/U, the Hubbard repulsion is the largest scale in the problem and hence states with double occupancies are projected out of the low-energy sector.

A Schrieffer-Wolff type canonical transformation, e^{-iS} [29] can then be used to perturbatively include effects of virtual transitions to the high-energy sector (with finite double occupancies). The transformation is obtained by assuming that the transformed Hamiltonian $\tilde{H} = e^{iS} H e^{-iS}$ does not have any term connecting low- and high-energy sectors. To first order in t/U,

$$iS = \sum_l \frac{T^1_{AB}(l) - T^{-1}_{BA}(l)}{U+V} + \frac{T^1_{BA}(l) - T^{-1}_{AB}(l)}{U-V}, \qquad (2)$$

where $T^{\eta}_{AB}(l)$ is the part of the hopping operator on the bond l which hops a fermion from A to B sublattice. and increases the double occupancy of the system by $\eta = 0, 1$, or -1. At half filling, the effective low-energy Hamiltonian is given by

$$\tilde{H} = \frac{J}{1 - \frac{V^2}{U^2}} \sum_{\langle ij \rangle} \left(\vec{S}_i \cdot \vec{S}_j - \frac{1}{4} n_i n_j \right), \qquad (3)$$

where the spin operator $\vec{S}_i = c^{\dagger}_{i\sigma} \vec{\sigma}_{\sigma\sigma'} c_{i\sigma'}$, and $J = 4t^2/U$ [14] is the standard Heisenberg superexchange scale. Physically,

there are two possible processes leading to the spin-spin interaction, one in which the double occupancy in the intermediate virtual state is formed on the B sublattice, and the other where it is formed on the A sublattice. They contribute with the scale $\sim t^2/(U \pm V)$ respectively, leading to an enhancement of the superexchange scale for small V/U. This can be contrasted with the extended Hubbard model with nearest neighbor interaction (which does not break sublattice symmetry), where the effective superexchange coupling increases with the nearest neighbor interaction V' as $\sim t^2/(U - V')$ [30,31]. In the strongly interacting limit of the Hubbard model ($V = 0$) at half filling, the Neel temperature scales with the Heisenberg coupling J, with numerical simulations yielding $T_N/J \sim 0.957$ on the cubic lattice [32]. The same scaling should hold in the small V/U limit, where the low-energy subspace does not contain any configuration with double occupancy, explaining the increase of T^N with V/t for small V/U. This finding is of great significance to the cold atom experiments, where an increased Neel temperature would lead to an easier detection of the AF ordered state, as the current OLE experiments on the standard fermionic Hubbard model are having difficulties reaching the $T < T^N$ regime.

The perturbative argument, which predicts a divergent superexchange coupling at $V = U$, breaks down as V/U approaches unity. The DMFT results for T^N as a function of V/t (see Fig. 2), however, show that for the strongly interacting system, T^N continues its rise up to $V/U \sim 0.6$, and the optimum T^N is 40% higher than that of the standard Hubbard model for $U/t = 16$.

In the ionic Hubbard model, when $V/U \sim 1$, the potential energy gained by fermions on the A sublattice can compensate for the energy cost of forming a double occupancy (as long as it is formed on the A sublattice). Thus the state $|\uparrow_A, \downarrow_B\rangle$ and the state $|\uparrow_A\downarrow_A, 0_B\rangle$ will have similar energies differing by $\sim U - V$. For $U - V \sim J$, these states lie in the low-energy subspace of the system and the Hubbard model can no longer be reduced to a simple Heisenberg model even at half filling. This picture is supported by the fact that the sublattice density asymmetry, $\Delta n = n_A^{\uparrow} + n_A^{\downarrow} - n_B^{\uparrow} - n_B^{\downarrow}$, remains constant up to T^N for small V/U, while for $V/U \sim 1$, it rapidly rises with temperature from a low-temperature asymptotic value to a constant high-temperature value beyond the Neel transition. This is clearly seen in Fig. 1(b). At half filling, Δn is a measure of the relative weight of doubly occupied states in the thermal ensemble, with $\Delta n = 0$ for states in the projected subspace, while $\Delta n = 2$ for the state with perfect density order, double occupancies on sublattice A, and vacancies on sublattice B. The temperature dependence of the density asymmetry shows that at small V/U, configurations with double occupancies do not play a major role in spin disordering, while at large V/U the loss of AF order is driven by the increasing presence of such configurations.

The loss of AF ordering due to inclusion of double occupancies results in an apparently counterintuitive phenomenon. As V is increased close to U, the low-energy single-particle DOS shows spin polarization, which initially increases with increasing temperature, before vanishing at the AF transition point. Thus, the system exhibits static AF order, but the low-energy dynamics of the system is very similar to a ferromagnet. Specifically, if a current is set up in the system, it will be carried by spin-polarized carriers and the system would show a finite spin conductivity even in the absence of a magnetic field. To see this, we compute the zero-frequency DOS for the fermions on a given sublattice and with a given spin from the imaginary-time Green's functions through

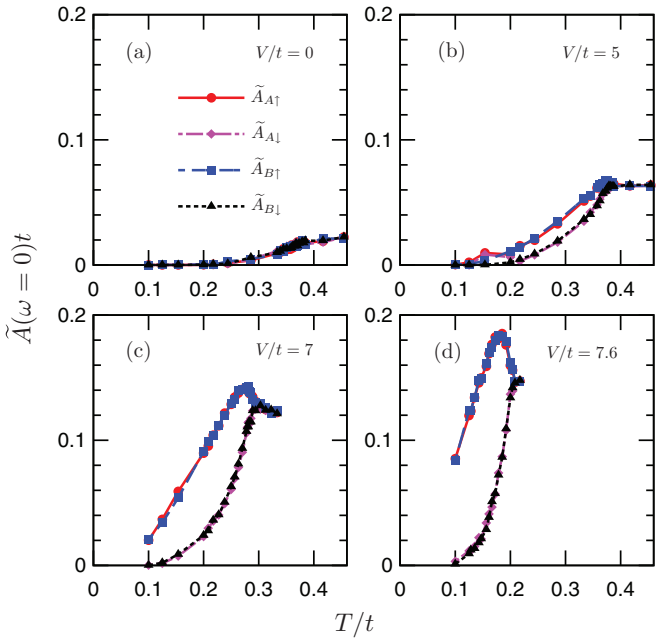

FIG. 3. (Color online) Estimated zero-frequency single-particle DOS $\tilde{A}(\omega = 0)$ of $\uparrow$ and $\downarrow$ spin particles on A and B sublattices, as a function of temperature for (a) $V/t = 0$, (b) $V/t = 5.0$, (c) $V/t = 7.0$, and (d) $V/t = 7.6$. The Hubbard interaction is fixed at $U/t = 10$ for all the plots. As V/t increases, the $\uparrow$ spin DOS shows a marked increase over the $\downarrow$ spin DOS.

$$\tilde{A}_{\sigma\alpha}(\omega = 0) = -\frac{1}{\pi T} G_{\alpha}^{\sigma}\left(\tau = \frac{1}{2T}\right). \tag{4}$$

This approximation to the zero-frequency density of states has been frequently used to determine the metallic vs insulating nature of the system [33]. In Fig. 3, we plot the zero-energy density of states for fermions of both spins on both sublattices as a function of temperature for (a) $V/t = 0$, (b) $V/t = 5$, (c) $V/t = 7$, and (d) $V/t = 7.6$ for a system with $U/t = 10$. Up to $V/t = 5$, we see very little spin asymmetry in the DOS, while for V/t larger than 7, there is a large asymmetry in the zero-energy DOS of the $\uparrow$ and $\downarrow$ spins. This asymmetry grows with temperature, and reaches a peak close to the transition before vanishing at the transition. Thus, the system is metallic at these temperatures, with transport and low-energy dynamics dominated by $\uparrow$ spins.

To understand the mechanism of spin polarization of low-energy DOS, we consider the extreme case of a perfectly Neel ordered state with $\downarrow$ spins on the A sublattice and $\uparrow$ spins on the B sublattice. As V/U is increased close to unity, the $\uparrow$ spin on the B sublattice can move to the A sublattice to form a double occupancy and keep the state in the low-energy subspace. However, the $\downarrow$ spin on the A sublattice cannot

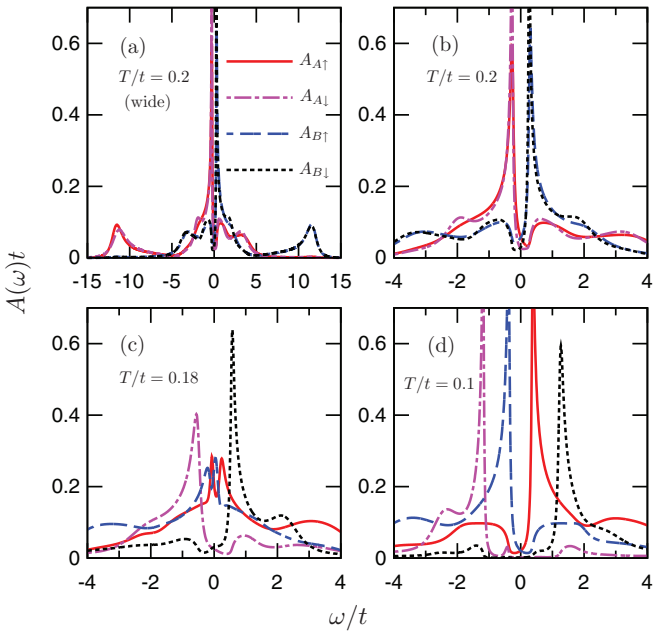

FIG. 4. (Color online) DOS of ↑ and ↓ spins on A and B sublattices, calculated by maximum entropy method, as a function of energy for $V/t = 7$ and $U/t = 10$. (a) Results for $T/t = 0.2$; (b) low-energy results for the same temperature. (c) Low-energy results for $T/t = 0.18$. (d) Low-energy results for $T/t = 0.1$.

move to the B sublattice, as the resulting state would have a high energy $\sim U + V$. These processes are thus prohibited to $O(t)$ and can only happen with a scale $O[t^2/(U + V)]$. Thus the low-energy dynamics is mainly the dynamics of the ↑ spins in this case. Once this basic mechanism is understood, one can generalize to more complicated states, but as long as the AF ordering is present, the low-energy density of states would be dominated by the majority spins on the B sublattice. The spin polarization of the low-energy density of states is thus understood as a consequence of a resonance between a projected AF ordered state and a state with double occupancy on the A sublattice. This shows the role of double occupancies in the degradation of AF ordering in the ionic Hubbard model for $V/U \sim 1$.

To study the energy dependence of the spin asymmetry in DOS, we analytically continue the Matsubara Green's functions to the real frequency domain and obtain the frequency-dependent spectral weight (spin and sublattice resolved), using the method of Ref. [34]. The results are plotted in Fig. 4 for a system with $U/t = 10$ and $V/t = 7$ for three different temperatures. In Fig. 4(b) we plot the results at a temperature of $T/t = 0.2$, which is above the AF transition temperature. Each sublattice shows complete symmetry between ↑ and ↓ spins in terms of the spectral weight. The asymmetry between A and B sublattices reflects the different densities on these sublattices. In Fig. 4(c), we plot the results for a temperature $T/t = 0.18$, which is just below the transition temperature, and where the spin asymmetry of the zero-frequency DOS, as seen in Fig. 3(c), is maximal. In this case, we clearly see a buildup of low-energy DOS for the ↑ spin, while the ↓ spin DOS shows a soft gap. Finally in Fig. 4(d), we plot the low-temperature results at $T/t = 0.1$. In this case, the ↑ spin DOS shows a soft gap, while the ↓ spin DOS shows a hard gap in the spectrum.

In conclusion, we have studied the ionic fermionic Hubbard model using DMFT. This model can be easily implemented in cold atom optical lattice systems and has a higher Neel temperature for AF transition than the standard Hubbard model for an accessible region in the parameter space. For small V/U, the effective superexchange scale, given by $4t^2/(U - V^2/U)$, increases with the ionic potential V. As a consequence, T^N increases with V/U, reaches an optimum value around $V/U \sim 0.6$, and then goes down with further increase in V/U. The optimum temperature is about 40% higher than that of the standard Hubbard model for $U/t = 16$, which should help in observing superexchange-dominated AF ordering in OLE experiments. At large $V/U \sim 1$, the AF order is degraded by inclusion of more and more configurations with double occupancies (on the A sublattice) in the ensemble. A consequence of this mechanism is the surprising result that the low-energy density of states shows strong spin asymmetry in the AF phase. Thus, with respect to dynamics and transport, the system behaves like a ferromagnet, although it shows static AF spin ordering. This novel feature of the ionic Hubbard model should manifest itself in the optical lattice emulation experiments.

The authors thank M. Randeria, H. R. Krishnamurthy, and K. Sengupta for fruitful discussions. This work is supported by the NSF-JQI-PFC, AFOSR MURI, and ARO MURI. The DMFT code is developed based on the ALPS library [35]. The computations are conducted at the Center for Nanophase Materials Sciences, which is sponsored at Oak Ridge National Laboratory by the Scientific User Facilities Division, Office of Basic Energy Sciences, US Department of Energy.

[1] I. Bloch, J. Dalibard, and W. Zwerger, Rev. Mod. Phys. **80**, 885 (2008).

[2] M. Greiner, O. Mandel, T. Esslinger, T. W. Hensch, and I. Bloch, Nature **415**, 39 (2002).

[3] R. Jördens, N. Strohmaier, K. Günter, H. Moritz, and T. Esslinger, Nature **455**, 204 (2008); D. Greif, T. Uehlinger, G. Jotzu, L. Tarruell, and T. Esslinger, Science **340**, 1307 (2013).

[4] U. Schneider *et al.*, Science **322**, 1520 (2008).

[5] W. S. Bakr, A. Peng, M. E. Tai, R. Ma, J. Simon, J. I. Gillen, S. Foelling, L. Pollet, and M. Greiner, Science **329**, 547 (2010).

[6] M. P. A. Fisher, P. B. Weichman, G. Grinstein, and D. S. Fisher, Phys. Rev. B **40**, 546 (1989).

[7] P. W. Anderson, Science **235**, 1196 (1987).

[8] S. Trotzky, P. Cheinet, S. Flling, M. Feld, U. Schnorrberger, A. M. Rey, A. Polkovnikov, E. A. Demler, M. D. Lukin, and I. Bloch, Science **319**, 295 (2008).

[9] F. Werner, O. Parcollet, A. Georges, and S. R. Hassan, Phys. Rev. Lett. **95**, 056401 (2005); R. Jordens, L. Tarruell, D. Greif, T. Uehlinger, N. Strohmaier, H. Moritz, T. Esslinger, L. De Leo, C. Kollath, A. Georges, V. Scarola, L. Pollet, E. Burovski, E. Kozik, and M. Troyer, *ibid*. **104**, 180401 (2010).

[10] P. Medley, D. M. Weld, H. Miyake, D. E. Pritchard, and W. Ketterle, Phys. Rev. Lett. **106**, 195301 (2011); W. S. Bakr, P. M. Preiss, M. E. Tai, R. Ma, J. Simon, and M. Greiner, Nature **480**, 500 (2011).

[11] J. Simon, W. S. Bakr, R. Ma, M. E. Tai, P. M. Preiss, and M. Greiner, Nature **472**, 307 (2011).

[12] S. Sachdev, K. Sengupta, and S. M. Girvin, Phys. Rev. B **66**, 075128 (2002).

[13] M. J. Rice and E. J. Mele, Phys. Rev. Lett. **49**, 1455 (1982).

[14] N. Nagaosa and J. Takimoto, J. Phys. Soc. Jpn **55**, 2735 (1986).

[15] W. S. Bakr, J. I. Gillen, A. Peng, S. Flling, and M. Greiner, Nature **462**, 74 (2009).

[16] J. T. Stewart, J. P. Gaebler, and D. S. Jin, Nature **454**, 744 (2008).

[17] A. Sommer, M. Ku, G. Roati, and M. W. Zwierlein, Nature **472**, 201 (2011).

[18] L. W. Cheuk, A. T. Sommer, Z. Hadzibabic, T. Yefsah, W. S. Bakr, and M. W. Zwierlein, Phys. Rev. Lett. **109**, 095302 (2012).

[19] T. Wilkens and R. M. Martin, Phys. Rev. B **63**, 235108 (2001).

[20] M. C. Refolio, J. M. Lopez Sancho, and J. Rubio, Phys. Rev. B **72**, 035121 (2005).

[21] A. Garg, H. R. Krishnamurthy, and M. Randeria, Phys. Rev. Lett. **97**, 046403 (2006).

[22] N. Paris, K. Bouadim, F. Hebert, G. G. Batrouni, and R. T. Scalettar, Phys. Rev. Lett. **98**, 046403 (2007).

[23] S. S. Kancharla and E. Dagotto, Phys. Rev. Lett. **98**, 016402 (2007).

[24] A. A. Aligia, Phys. Rev. B **69**, 041101(R) (2004).

[25] K. Byczuk, M. Sekania, W. Hofstetter, and A. P. Kampf, Phys. Rev. B **79**, 121103(R) (2009).

[26] A. Garg, H. R. Krishnamurthy, and M. Randeria, Phys. Rev. Lett. **112**, 106406 (2014).

[27] A. Georges, G. Kotliar, W. Krauth, and M. J. Rozenberg, Rev. Mod. Phys. **68**, 13 (1996); G. Kotliar, S. Y. Savrasov, K. Haule, V. S. Oudovenko, O. Parcollet, and C. A. Marianetti, *ibid*. **78**, 865 (2006).

[28] E. Gull, A. J. Millis, A. I. Lichtenstein, A. N. Rubtsov, M. Troyer, and P. Werner, Rev. Mod. Phys. **83**, 349 (2011).

[29] A. H. MacDonald, S. M. Girvin, and D. Yoshioka, Phys. Rev. B **37**, 9753 (1988).

[30] A. E. Ruckenstein, P. J. Hirschfeld, and J. Appel, Phys. Rev. B **36**, 857 (1987).

[31] P. G. J. van Dongen, Phys. Rev. B **49**, 7904 (1994).

[32] R. Staudt, M. Dzierzawa, and A. Muramatsu, Eur. Phys. J. B **17**, 411 (2000).

[33] N. Trivedi and M. Randeria, Phys. Rev. Lett. **75**, 312 (1995); E. Gull, P. Werner, X. Wang, M. Troyer, and A. J. Millis, Europhys. Lett. **84**, 37009 (2008); E. Gull, M. Ferrero, O. Parcollet, A. Georges, and A. J. Millis, Phys. Rev. B **82**, 155101 (2010).

[34] X. Wang, E. Gull, L. de'Medici, M. Capone, A. J. Millis, Phys. Rev. B **80**, 045101 (2009).

[35] A. F. Albuquerque *et al*., J. Magn. Magn. Mater. **310**, 1187 (2007); B. Bauer *et al*., J. Stat. Mech. Theor. Exp. (2011) P05001.